Biochemistry (Moscow), Vol. 64, No. 7, 1999, pp. 832-838. Translated from Biokhimiya, Vol. 64, No. 7, 1999, pp. 990-997.

Modeling of Irreversible Thermal Protein Denaturation at Varying Temperature. II. The Complete Kinetic Model of Lumry and Eyring

A. E. Lyubarev* and B. I. Kurganov

Bach Institute of Biochemistry, Russian Academy of Sciences, Leninskii pr. 33, Moscow, 117071 Russia; fax: (095) 954-2732; E-mail: inbio@glas.apc.org

Received November 13, 1998
Revision received December 7, 1998

Abstract—The model for thermal denaturation of proteins involving consecutive reversible and irreversible steps (Lumry and Eyring model) has been analyzed. The most general case, when equilibrium in the first step is established slowly in comparison with the rate of the second step and the heat effect value for the second step is either greater than or less than zero, has been considered. The theoretical dependences of excess heat capacity on temperature have been constructed. The variation of the shape of the theoretical curves with varied values of the enthalpy change for the second step, Arrhenius equation parameters for both steps, and the scanning rate has been studied.

Key words: protein denaturation, Lumry and Eyring model, Arrhenius equation, differential scanning calorimetry

Differential scanning calorimetry (DSC) is widely used to study thermal denaturation of proteins. Mathematical analysis of the dependences of protein heat capacity (C_p) on temperature (T) allows the thermodynamic and kinetic characteristics of denaturation to be established [1-4].

The mathematical apparatus for analysis of DSC data has been elaborated in detail for mechanisms of reversible equilibrium protein denaturation [1-3]. However, it is known that many proteins denature irreversibly during calorimetrical experiments [3, 4]. To interpret the DSC data in such cases, special analytical methods are needed.

The simplest model of irreversible denaturation is the model including one irreversible step. Mathematical methods for analysis of DSC data for proteins that denature according to this model have been published by Sanchez-Ruiz and coauthors [5-7]. However, the one-step model has been shown to inadequately describe the irreversible denaturation of several proteins [7-9].

* To whom correspondence should be addressed.

It is generally accepted that protein denaturation can be described by the Lumry and Eyring model [10]; it includes consecutive reversible and irreversible steps:

$$N \underset{k_{-1}}{\overset{k_1}{\rightleftharpoons}} U \xrightarrow{k_2} D, \qquad (1)$$

where N, U, and D are native, partially unfolded, and denatured states of a protein and k_1, k_{-1}, and k_2 are the rate constants of the corresponding reactions. Attempts have been made to use this model for description of the denaturation of certain proteins [8, 11-15].

In the present work a theoretical analysis of protein DSC curves following this model is given for various parameter values.

LUMRY AND EYRING MODEL AND ITS PARTICULAR CASES

At constant scanning rate $v = dT/dt$ (T is absolute temperature, t is time) the kinetic behavior of the system described by model (1) is determined by the system of differential equations:

0006-2979/99/6407-0832$22.00 ©1999 МАИК "Наука/Interperiodica"

$$\begin{cases} \dfrac{d\gamma_N}{dT} = \dfrac{1}{v}(k_{-1}\gamma_U - k_1\gamma_N) \\ \dfrac{d\gamma_U}{dT} = \dfrac{1}{v}(k_1\gamma_N - k_2\gamma_U - k_{-1}\gamma_U) \end{cases}, \quad (2)$$

where γ_N and γ_U are the mole fractions of native and partially unfolded protein, respectively. This system of equations does not have an analytical solution.

The dependences of rate constants of individual steps (k_1, k_{-1}, and k_2) on temperature follow the Arrhenius equation. It is convenient to write this equation in the following form:

$$k = \exp\left\{\frac{E_a}{R}\left[\frac{1}{T^*} - \frac{1}{T}\right]\right\}, \quad (3)$$

where E_a is the energy of activation, R is the gas constant, and T^* is the temperature at which rate constant equals 1 min^{-1}.

The excess enthalpy change of the reaction $\langle\Delta H\rangle$ is the sum of the excess enthalpy changes for both steps:

$$\langle\Delta H\rangle = \Delta H_1(1 - \gamma_N) + \Delta H_2(1 - \gamma_N - \gamma_U), \quad (4)$$

where ΔH_1 and ΔH_2 are molar enthalpy changes for the first and second steps, respectively. Taking into consideration the system of equations (2), the excess heat capacity is expressed by the equation:

$$C_p^{ex} = \frac{d\langle\Delta H\rangle}{dT} = \frac{\Delta H_1}{v}(k_1\gamma_N - k_{-1}\gamma_U) + \frac{\Delta H_2}{v}k_2\gamma_U. \quad (5)$$

The dependences of γ_N and γ_U on temperature for each set of the parameters can be determined by numerical solution of the system of differential equations (2).

Taking into consideration that the enthalpy change for the first step and the energies of activation for the direct and reverse reactions are connected by the relationship $\Delta H = E_{a,1} - E_{a,-1}$, we conclude that the shape of the excess heat capacity C_p^{ex} versus temperature curve is determined by the scanning rate v and seven parameters of the denaturation process: the energy of activation and the parameter T^* for each of three reactions and the enthalpy change for the second step.

Both one-step reversible and one-step irreversible models can be considered as particular cases of the Lumry and Eyring model [16]. The first case is realized if the rate of the second step is sufficiently small and the form N is transformed to form U without considerable conversion of the later to form D. The second case is possible when the rate of the second step is sufficiently large and the direct reaction of the first step is the rate-limiting one and the reverse reaction is practically absent.

A more complex particular case of the Lumry and Eyring model is the model involving two consecutive irreversible steps:

$$N \xrightarrow{k_1} U \xrightarrow{k_2} D. \quad (6)$$

This model is realized for the situation when the rate of the reverse reaction of the first step is much less than the rate of the second step. Unlike the one-step irreversible model, in this case the rate of the direct reaction of the first step is comparable with the rate of the second step. Theoretical analysis of this model has been given in [17]. Using this model, we described the thermal denaturation of uridine phosphorylase from *Escherichia coli* [18, 19].

The Lumry and Eyring model with fast equilibrating first step can be considered as another particular case of the complete kinetic model of Lumry and Eyring. This model has been analyzed in [11, 20]. The model has been used for description of the thermal denaturation of azurin from *Pseudomonas aeruginosa* [11-13].

The complete kinetic model of Lumry and Eyring was studied in relation to DSC data only in the work of Lepock and coauthors [16]. However, they analyzed only the situation when the second step is not accompanied by a heat effect ($\Delta H_2 = 0$). Also, the effect of only one parameter (T_2^*) on the shape of DSC curves was studied in that work. In the present work more extensive study of the Lumry and Eyring model has been undertaken.

METHOD OF INVESTIGATION

For calculation of model curves describing the dependence of excess heat capacity (C_p^{ex}) on temperature according to Eqs. (2), (3), and (5), we used the commercial software Scientist (MicroMath Inc., USA). In all the cases the ΔH_1 value is taken equal to 400 kJ/mole (as in [16]) and the T_1^* value is taken equal to 328.16 K (55°C). Values of the other parameters are varied.

RESULTS AND DISCUSSION

Effect of the parameter T_2^* on the shape of profiles of excess heat capacity versus temperature. Let us first consider the simplest case of the Lumry and Eyring model when the heat effect of the second step is absent ($\Delta H_2 = 0$) and the energy of activation for the second step equals the energy of activation for the direct reaction of the

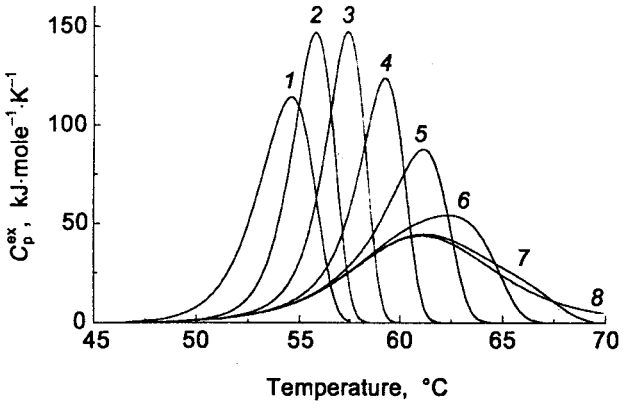

Fig. 1. Temperature profiles of excess heat capacity (C_p^{ex}) at various values of parameter T_2^*. For all curves $E_{a,1} = E_{a,2} =$ 685 kJ/mole, $E_{a,-1} =$ 285 kJ/mole, $\Delta H_1 =$ 400 kJ/mole, $\Delta H_2 =$ 0, $T_1^* =$ 328.16 K (55°C), $T_{-1}^* =$ 319.92 K, $v =$ 1 deg/min. The values of T_2^* (in parentheses the ratio of constants k_1/k_2 is given at the temperature at which the equilibrium constant equals unity): *1*) 316.5 K (10^{-4}); *2*) 325.2 K (0.1); *3*) 328.2 K (1); *4*) 331.2 K (10); *5*) 334.3 K (100); *6*) 337.4 K (1000); *7*) 340.7 K (10^4); *8*) 347.3 K (10^6).

first step ($E_{a,1} = E_{a,2}$). The values of the later are taken equal to 685 kJ/mole (as in [16]). The value of scanning rate is taken equal to 1 deg/min; the values of parameters T_1^* and T_{-1}^* (328.16 and 319.92 K) are taken in such a way that the temperature (T_m) at which the equilibrium constant equals unity is 334 K (61.1°C) and the k_1 and k_{-1} values at this temperature are 100 min^{-1}.

Figure 1 shows the profiles of C_p^{ex} versus T at various values of parameter T_2^*. An analogous set of profiles was given in [16]. Curve *1* corresponds to the value of parameter T_2^* for which the ratio k_1/k_2 at temperature T_m equals 10^{-4}. In this case the kinetic behavior of the system is determined only by the rate of the direct reaction of the first step, and the Lumry and Eyring model is reduced to the one-step irreversible model. Indeed, curve *1* coincides with the curve constructed for the one-step model at the values of the parameters corresponding to the values of the parameters of the direct reaction of the first step.

Curve *8* corresponds to the value of parameter T_2^* for which the ratio k_1/k_2 at temperature T_m equals 10^6. In this case the second step is practically absent, and the Lumry and Eyring model is reduced to the one-step reversible model. Curve *7* (the ratio k_1/k_2 at temperature T_m equals 10^4) differs only little from curve *8*; only the descending part is slightly steeper.

Curves *2-6* correspond to the values of parameter T_2^* for which the ratio k_1/k_2 at temperature T_m varies from 0.1 to 1000. In these cases the kinetic behavior of the system is determined by all three reactions.

Figure 2 shows (for four values of parameter T_2^*) how fractions of the forms N, U, and D change with temperature. It is obvious that, in the case of the ratio k_1/k_2 at temperature T_m of 10^{-4}, there is no accumulation of form U (a). At the ratio k_1/k_2 of unity, form U is accumulated in relatively small amounts (b). In the case of the ratio k_1/k_2 of 1000 there is a significant accumulation of the intermediate (c). At the ratio k_1/k_2 of 10^6, conversion of form U to form D is not observed until practically all native protein N is transformed to the partially unfolded form U (d).

The degree of peak asymmetry is an important visual characteristic of the DSC curve. This degree can be defined as the ratio of heat absorbed before the maximum point to the heat absorbed after this point (i.e., the ratio of areas of the left and right parts of the peak) [17, 21]. For DSC curves following the one-step model this ratio equals 1.7 [17, 21]. We obtained the same value for curve *1* in Fig. 1. For curve *2* the degree

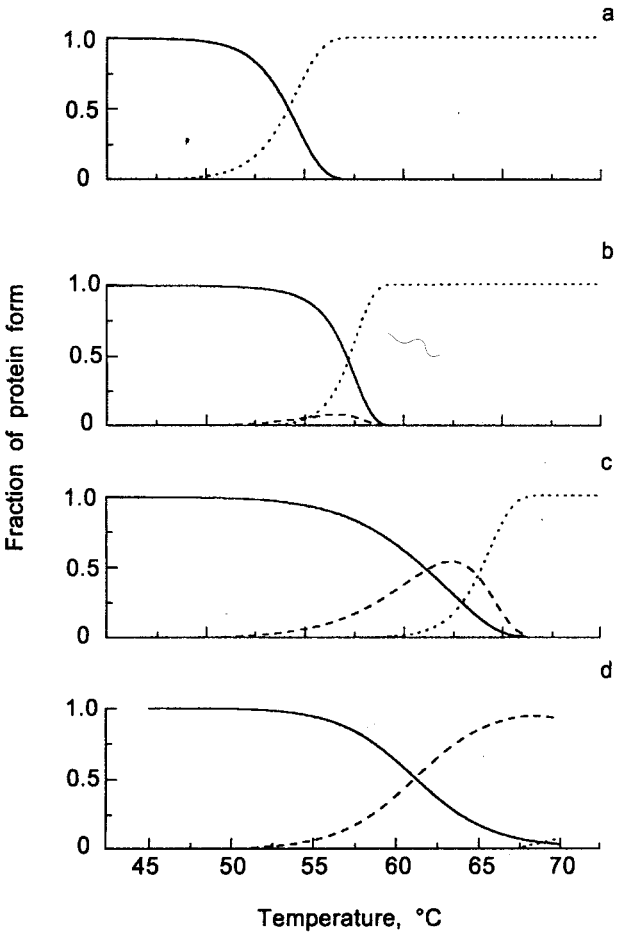

Fig. 2. Temperature dependences of fractions of the native form of a protein (N) and the form of a protein arising in the course of denaturation: partially unfolded (U) and denatured (D). For all the curves $E_{a,1} = E_{a,2} =$ 685 kJ/mole, $E_{a,-1} =$ 285 kJ/mole, $\Delta H_1 =$ 400 kJ/mole, $\Delta H_2 =$ 0, $T_1^* =$ 328.16 K (55°C), $T_{-1}^* =$ 319.92 K, $v =$ 1 deg/min. The values of T_2^* (in the parentheses the ratio of constants k_1/k_2 is given at the temperature at which the equilibrium constant equals unity): a) 316.5 K (10^{-4}); b) 328.2 K (1); c) 337.4 K (1000); d) 347.3 K (10^6).

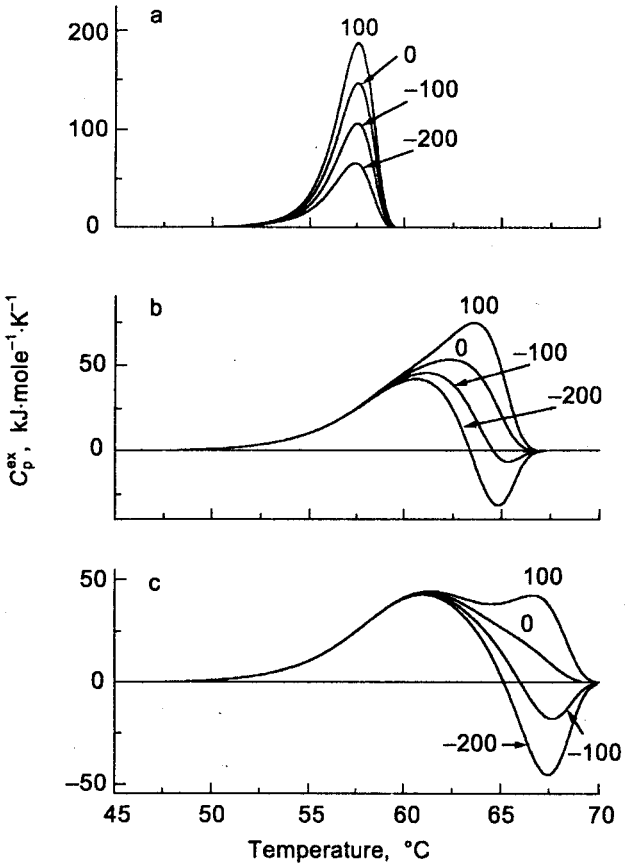

Fig. 3. Temperature profiles of excess heat capacity at various values of the enthalpy change for the second step. For all the curves $E_{a,1} = E_{a,2} = 685$ kJ/mole, $E_{a,-1} = 285$ kJ/mole, $\Delta H_1 = 400$ kJ/mole, $T_{\frac{1}{2}}^* = 328.16$ K (55°C), $T_{\frac{1}{2}}^*{}_{-1} = 319.92$ K, $v = 1$ deg/min. The values of $T_{\frac{1}{2}}^*$ (in the parentheses the ratio of constants k_1/k_2 is given at the temperature at which the equilibrium constant equals unity): a) 328.2 K (1); b) 337.4 K (1000); c) 340.7 K (10^4). The values of ΔH_2 (kJ/mole) are shown above the curves.

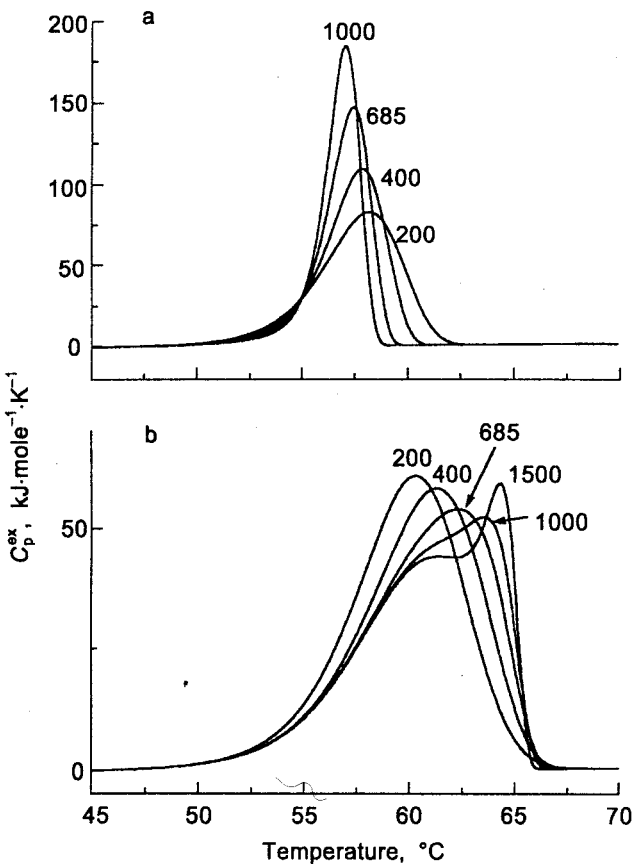

Fig. 4. Temperature profiles of excess heat capacity at various values of the energy of activation for the second step. For all the curves $E_{a,1} = 685$ kJ/mole, $E_{a,-1} = 285$ kJ/mole, $\Delta H_1 = 400$ kJ/mole, $\Delta H_2 = 0$, $T_{\frac{1}{2}}^* = 328.16$ K (55°C), $T_{\frac{1}{2}}^*{}_{-1} = 319.92$ K, $v = 1$ deg/min. The values of $T_{\frac{1}{2}}^*$ (in the parentheses the ratio of constants k_1/k_2 is given at the temperature at which the equilibrium constant equals unity): a) 328.2 K (1); b) 337.4 K (1000). The values of $E_{a,2}$ (kJ/mole) are shown above the curves.

of asymmetry also equals 1.7, for curve *3* it equals 1.8, and for curve *4* it equals 2.0. Curves *5* and *6* are the most asymmetrical (2.4 and 2.2, respectively). As for curves *7* and *8*, their degrees of asymmetry equal 1.0, as is typical of the one-step reversible model.

Effect of the enthalpy change for the second step on the shape of profiles of excess heat capacity versus temperature. Let us now consider the case when the second step of denaturation is accompanied by a significant heat effect. The second step can be endothermic ($\Delta H_2 > 0$) or exothermic ($\Delta H_2 < 0$).

Figure 3 shows the profiles of C_p^{ex} versus T at various values of ΔH_2. It is obvious that, in the case when the accumulation of the intermediate U is small (a), the value of enthalpy change does not significantly effect the shape of the curves (the degree of asymmetry slightly increases for the exothermic case: 2.0 at $\Delta H_2 = -200$ kJ/mole).

When the intermediate is accumulated in significant amounts (b, c), the effect of the value of enthalpy change on the shape of the C_p^{ex} versus T profiles becomes considerable. In the exothermic case a negative peak at rather high temperatures appears. In the endothermic case the appearance of a second positive peak can be observed (c). The cause is that the maximum values of the rates for the first and second steps are reached in different temperature ranges.

Effect of the value of the energy of activation for the second step on the shape of profiles of excess heat capacity versus temperature. Let us now consider the case when the energy of activation for the second step differs from that for the direct reaction of the first step. Figure 4 shows the profiles of C_p^{ex} versus T at various values of $E_{a,2}$. When accumulation of the intermediate U is small (a), the effect of the value of the energy of activation for the second step consists in the change of peak width (the greater $E_{a,2}$, the narrower the peak) and in some shift of the maximum point (the greater $E_{a,2}$, the lower the temperature of

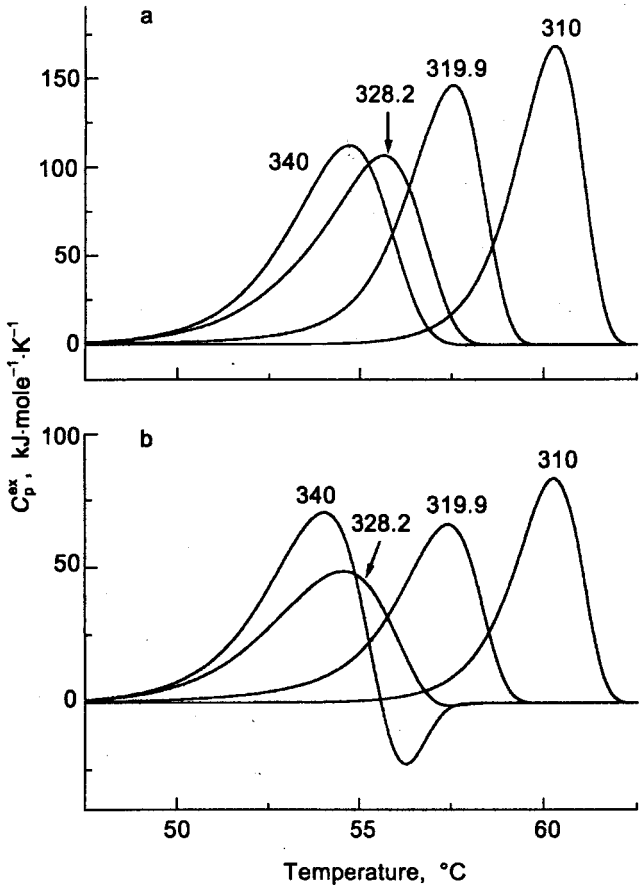

Fig. 5. Temperature profiles of excess heat capacity for various values of parameter T^*_{-1}. For all the curves $E_{a,1}$ = $E_{a,2}$ = 685 kJ/mole, $E_{a,-1}$ = 285 kJ/mole, ΔH_1 = 400 kJ/mole, T^*_1 = T^*_2 = 328.16 K (55°C), v = 1 deg/min. The values of ΔH_2: 0 (a), –200 kJ/mole (b). The values of parameter T^*_{-1} (K) are shown above the curves.

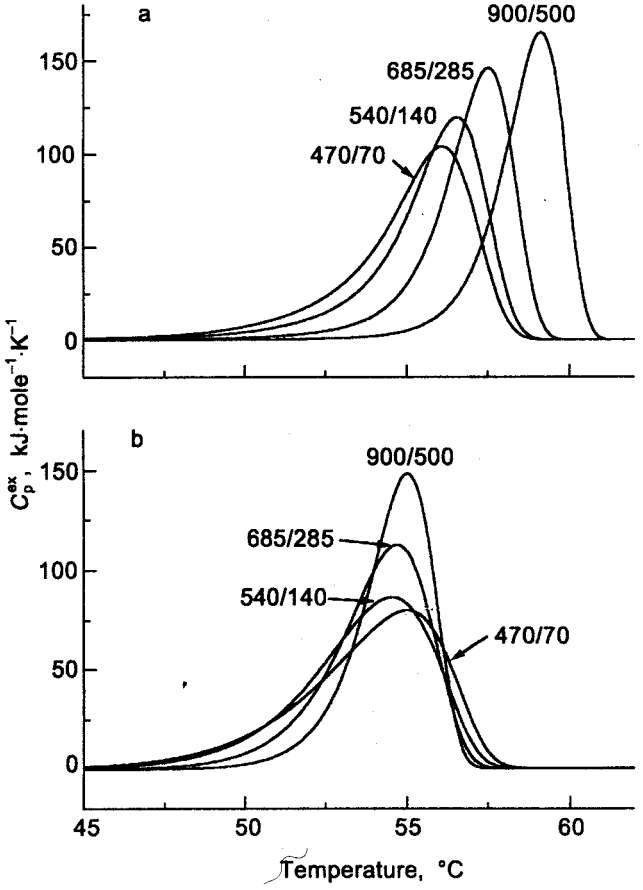

Fig. 6. Temperature profiles of excess heat capacity for various values of the energies of activation for the reactions of the first step. For all the curves ΔH_1 = 400 kJ/mole, ΔH_2 = 0, T^*_1 = T^*_2 = 328.16 K (55°C), v = 1 deg/min. The values of T^*_{-1}: 319.9 K (a), 340 K (b). The values of $E_{a,1}/E_{a,-1}$ (kJ/mole) are shown above the curves.

the maximum). The degree of peak asymmetry changes only slightly: from 1.6 for $E_{a,2}$ = 200 kJ/mole to 1.8 for $E_{a,2}$ = 1000 kJ/mole.

In the case when the intermediate is accumulated in significant amounts (b), the shape of the curve depends significantly on the value of the energy of activation for the second step. At $E_{a,2}$ = 200 kJ/mole, the curve is rather symmetrical (the degree of asymmetry is 1.4); at $E_{a,2}$ = 1000 kJ/mole, a sharp asymmetry is observed and an additional shoulder appears on the curve; at $E_{a,2}$ = 1500 kJ/mole, two peaks are distinctly seen on the curve.

Effect of the parameters of the reverse reaction on the shape of profiles of excess heat capacity versus temperature. Varying values of the parameter T^*_{-1} affect significantly the maximum point on the DSC curve (Fig. 5). Thus, at T^*_{-1} = 340 K (T^*_1 = T^*_2 = 328.2 K), the values of the rate constants k_1 and k_2 in the temperature range 50-57°C (323-330 K) are much higher than the value of the constant k_{-1}; therefore, in such case the Lumry and Eyring model is reduced to model (6) including only two consecutive irreversible steps.

When T^*_{-1} = 310 K, the rate constant for the reverse reaction is much higher than the rate constants of the direct reactions at relatively low temperature; therefore, denaturation starts at temperature higher than 55°C.

It should be noted that at T^*_{-1} = T^*_1 = T^*_2 = 328.2 K the peak is the most asymmetrical (the degree of asymmetry is 2.0, whereas at T^*_{-1} = 310 and 340 K the degree of asymmetry is 1.7) and the maximum value of excess heat capacity is less than the corresponding values for the curve obtained at both higher and lower values of parameter T^*_{-1} (Fig. 5a).

In the case of the exothermic second step (Fig. 5b), the negative peak appears only at T^*_{-1} = 340 K.

Change of the energies of activation for the direct and reverse reactions of the first step (with conserva-

tion of the value of their difference, i.e., the value of enthalpy change for the first step) affects differently the shape of the curves in coordinates $\{C_p^{ex}; T\}$ depending on the ratio between the values of parameters T^*_{-1} and T^*_2 (Fig. 6). Thus, at $T^*_{-1} < T^*_2$ (a), increasing the energy of activation results in a significant shift of the maximum point, increasing the maximum value of excess heat capacity and decreasing the degree of peak asymmetry (from 2.0 at 70 kJ/mole to 1.75 at 500 kJ/mole).

In the case when $T^*_{-1} > T^*_2$ (b), the position of the maximum does not significantly change. The maximum value of excess heat capacity increases with the energy of activation as well. At $E_{a,-1}$ = 70 kJ/mole, the peak is sharply asymmetrical (2.1); increasing the energy of activation from 140 to 500 kJ/mole has no significant effect on the degree of asymmetry (it is equal to C_p^{ex} 1.7).

Effect of the scanning rate on the shape of profiles of excess heat capacity versus temperature. A sensitivity of DSC profiles to the scanning rate is an essential characteristic of an irreversible thermal denaturation. In the case of the one-step model the shape of the profile practically does not change, but the point of the maximum is shifted towards higher temperatures with a small decrease of the maximum value of the excess heat capacity [3, 4].

In the case of the Lumry and Eyring model an analogous situation is possible when the rate of the second step is high and there is not significant accumulation of the intermediate (Fig. 7a). If the intermediate is accumulated, the effect of the scanning rate is revealed in the other way (Fig. 7, b and c). Thus, at the ratio k_1/k_2 of 1000 at temperature T_m (b) the maximum point shifts insignificantly with the scanning rate, whereas the maximum value of excess heat capacity decreases significantly, as well as the degree of asymmetry (from 2.4-2.5 at v = 0.125-0.5 deg/min to 1.5 at v = 2 deg/min). In the case of higher values of the energy of activation for the second step (c), an additional shoulder or second peak appears on the C_p^{ex} versus T profiles when the scanning rate increases.

In previous work we have shown that in the case of the model including two consecutive irreversible steps the scanning rate also significantly affects the shape of DSC curves [17]. However, the effect of the scanning rate for the two models is not identical. Thus, in the case of the model including two consecutive irreversible steps, at $E_{a,2} > E_{a,1}$ peak separation occurs more effectively at lower values of the scanning rate. Thus, a set of several excess heat capacity versus temperature profiles obtained at various scanning rates reveals information about the possible denaturation mechanism and allows a qualitative estimation of the ratio of the parameters of the process.

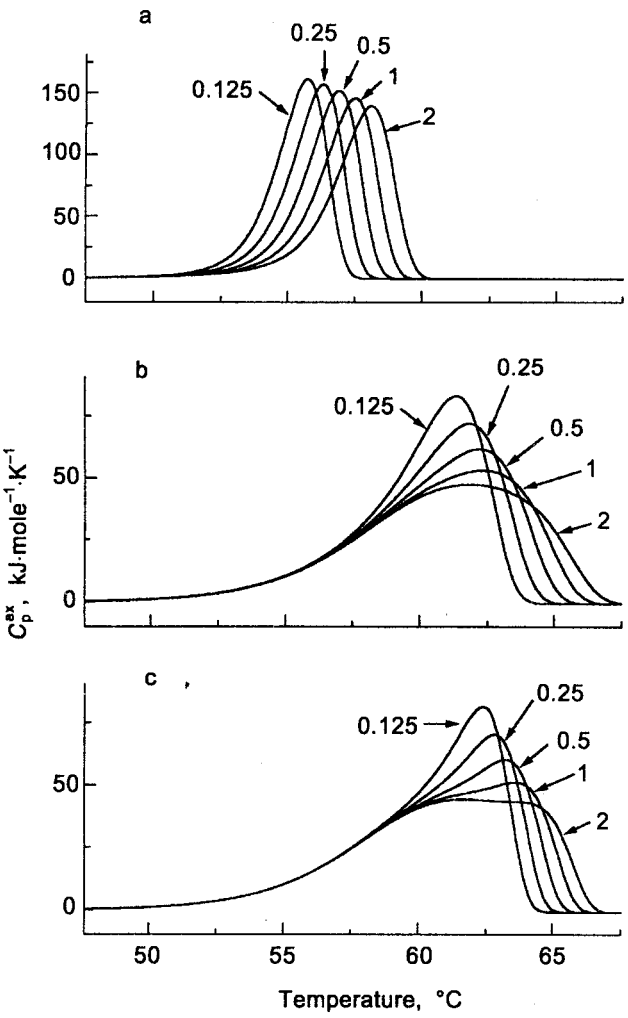

Fig. 7. Effect of the scanning rate on the shape of temperature profiles of excess heat capacity. For all the curves $E_{a,1}$ = 685 kJ/mole, $E_{a,-1}$ = 285 kJ/mole, ΔH_1 = 400 kJ/mole, ΔH_2 = 0, T^*_1 = 328.16 K (55°C), T^*_{-1} = 319.92 K. The values of $E_{a,2}$: 685 (a, b) and 1000 kJ/mole (c). The values of T^*_2 (in the parentheses the ratio of constants k_1/k_2 is given at the temperature at which the equilibrium constant equals unity): a) 328.2 K (1); b, c) 337.4 K (1000). The values of v (deg/min) are shown above the curves.

This work was supported by the Russian Foundation for Basic Research (grants 96-04-50819 and 96-04-10016C).

REFERENCES

1. Privalov, P. L., and Potekhin, S. A. (1986) *Meth. Enzymol.*, **131**, 4-51.
2. Sturtevant, J. M. (1987) *Annu. Rev. Phys. Chem.*, **38**, 463-488.
3. Freire, E., van Osdol, W. W., Mayorga, O. L., and Sanchez-Ruiz, J. M. (1990) *Annu. Rev. Biophys. Biophys. Chem.*, **19**, 159-188.

4. Sanchez-Ruiz, J. M. (1995) *Subcellular Biochemistry*, **24**, 133-176.
5. Sánchez-Ruiz, J. M., Lopéz-Lacomba, J. L., Cortijo, M., and Mateo, P. L. (1988) *Biochemistry*, **27**, 1648-1652.
6. Conejero-Lara, F., Sánchez-Ruiz, J. M., Mateo, P. L., Burgos, F. J., Vendrell, J., and Avilés, F. X. (1991) *Eur. J. Biochem.*, **200**, 663-670.
7. Kurganov, B. I., Lyubarev, A. E., Sánchez-Ruiz, J. M., and Shnyrov, V. L. (1997) *Biophys. Chem.*, **69**, 125-135.
8. Tello-Solis, S. R., and Hernandez-Arana, A. (1995) *Biochem. J.*, **311**, 969-974.
9. Davoodi, J., Wakarchuk, W. W., Surewicz, W. K., and Carey, P. R. (1998) *Protein Sci.*, **7**, 1538-1544.
10. Lumry, R., and Eyring, H. (1954) *J. Phys. Chem.*, **58**, 110-120.
11. Milardi, D., La Rosa, C., and Grasso, D. (1994) *Biophys. Chem.*, **52**, 183-189.
12. La Rosa, C., Milardi, D., Grasso, D., Guzzi, R., and Sportelli, L. (1995) *J. Phys. Chem.*, **99**, 14864-14870.
13. Guzzi, R., La Rosa, C., Grasso, D., Milardi, D., and Sportelli, L. (1996) *Biophys. Chem.*, **60**, 29-38.
14. Singh, N., Liu, Z., and Fisher, H. F. (1996) *Biophys. Chem.*, **63**, 27-36.
15. Vogl, T., Jatzke, C., Hinz, H.-J., Benz, J., and Huber, R. (1997) *Biochemistry*, **36**, 1657-1668.
16. Lepock, J. R., Ritchie, K. P., Kolios, M. C., Rodahl, A. M., Heinz, K. A., and Kruuv, J. (1992) *Biochemistry*, **31**, 12706-12712.
17. Lyubarev, A. E., and Kurganov, B. I. (1998) *Biochemistry (Moscow)*, **63**, 434-440.
18. Lyubarev, A. E., Kurganov, B. I., Burlakova, A. A., Orlov, V. N., and Poglazov, B. F. (1998) *Dokl. Ros. Akad. Nauk*, **358**, 830-832.
19. Lyubarev, A. E., Kurganov, B. I., Burlakova, A. A., and Orlov, V. N. (1998) *Biophys. Chem.*, **70**, 247-257.
20. Sanchez-Ruiz, J. M. (1992) *Biophys. J.*, **61**, 921-935.
21. Potekhin, S. A., and Kovrigin, E. L. (1998) *Biofizika*, **43**, 223-232.